Chain Length Effect on the Configurational Properties of an n-Alkane Chain in Solution

Seung Ho Jeon, and Taikyue Ree*

Department of Chemistry, Korea Advanced Institute of Science and Technology, Seoul 131

In Joon Oh

Department of Pharmacy, College of Pharmacy, Chunnam National University, Kwangju, Chunnam 500
Received June 21, 1986

Dynamic and equilibrium properties of n-alkane chains immersed in solvent molecules have been investigated by a molecular dynamics method. The n-alkane chain is assumed to be a chain of elements (CH_2) interconnected by bonds having a fixed bond length and bond angle, but each bond of the chain is allowed to execute hindered internal rotation. We studied the effect of the number of the chain elements ($N_c = 10, 15$ and 20) on the equilibrium properties of the system, e.g., the pair correlation functions between a chain element and solvent molecules, $g_{cs}(r)$, and between the chain elements, $g_{cc}(r)$, and the configurational properties such as the mean-square end-to-end distance $\langle R^2 \rangle$, the mean-square radius of gyration $\langle S^2 \rangle$, and the eigenvalues of the moment-of-inertia tensor $\langle S_i^2 \rangle / \langle S^2 \rangle$ ($i = 1, 2$ and 3). We also studied the dynamic properties of the system, e.g., the autocorrelation function $C(A;t)$ where $A = R^2(t)$, $= S^2(t)$, or $= \vec{V}(t)$ ($\vec{V} =$ velocity of the center of mass), and the diffusion coefficient D. The $g_{cs}(r)$'s are almost equal irrespective of the change of N_c while $g_{cc}(r)$ becomes larger as N_c increases; The MD computed configurational properties $\langle R^2 \rangle$ and $\langle S^2 \rangle$ were found to be a little different from the values calculated from the statistical equations of $\langle R^2 \rangle$ and $\langle S^2 \rangle$, it may be due to the fact that our model for the MD simulations includes a long-range volume effect. From the $\langle S_i^2 \rangle / \langle S^2 \rangle$, it is found that the chain molecule has a nearly spherical shape irrespective of the variation of N_c. For the dynamic properties we found that the $C(R^2;t)$ and $C(S^2;t)$ of lower N_c decay faster than those of higher N_c, while the $C(\vec{V};t)$ of the center of mass in the chain is weakly dependent on the N_c. The center of mass diffusion coefficient D_c decreases as N_c increases while the end point diffusion coefficient D_e is nearly equal irrespective of the change of N_c.

Introduction

Configurational properties of a chain molecule have been studied by computer simulations, and many authors found that the configurational properties are dependent on the number of chain elements. Baumgärtner[1] studied the static properties of the freely jointed chain by Monte Carlo method and found that the mean size of a polymer chain has an $N_c^{1/2}$ dependence, N_c being the number of chain elements. Stellman and Gans[2] simulated by Monte Carlo method for a hard-sphere linear polymer-chain and found that the end-to-end distance and the radius of gyration exhibit an exponential dependence on N_c. Ceperley et al.[3] have developed a dynamic Monte Carlo technique for the simulation of the dynamics of a single polymer chain in solution. They observed that the time dependent correlation functions are dependent on N_c ($5 \leqslant N_c \leqslant 63$ and $a \simeq 2.2$).

Verdier and Stockmayer[4] were the first workers to study the relaxation behavior of the chains by using a Monte Carlo technique, and found that the relaxation behavior depends on the number of chain elements. Similar studies using a molecular dynamics(MD) method were carried out by Bishop et al.[5] Rapaport,[6,7] and Lee and Ree.[8]

Bishop et al.[5] used a shifted Lennard-Jones potential which has no attractive part, and Rapaport[7] used a harmonic model.

Lee and Ree[8] used a Lennard-Jones potential to represent the interactions between various particles except for the interactions between two particles jointed by a chemical bond for which Hookean potentials were used.

However, the models for the chain in all of the works cited above have been based on the freely-jointed chain. Thus, in our laboratory, a more realistic model of a semirigid chain with hindered internal rotations has been used.[9-11] In this paper, the same model of hindered rotation-chain molecule has been adopted, but with different lengths of the molecule. From the results, we shall discuss the dependence of the number of chain elements on the configurational properties of the chain molecules in solution.

Experimental

We consider a system of an n-alkane chain molecule immersed in solvent particles. The $N(= 256)$ particles move in the cubic box in accordance with the Newton equation of motion. The pair potential between solvent-solvent particles (SS), between chain element-solvent particles (CS), and between two chain elements (CC) is expressed by the exp-6 potential,

$$V(r) = \frac{\varepsilon}{\alpha - 6} \{6 \exp[\alpha(1 - \frac{r}{r_m})] - \alpha(\frac{r_m}{r})^6\} \tag{1}$$

where r_m ($=0.36$ nm) is the distance at which V(r) becomes minimum, ε ($=0.3$ kcal/mole) is the depth of the potential, and α ($=14.0$) represents the stiffness of the repulsive part of the potential. These numerical values follow from our previous paper.[9]

The model of the chain molecule is the same as in our previous works,[9-11] i.e., the bond length and bond angle are kept fixed, and the rotational angle ϕ varies with the allowance of the rotational potential,

$$V(\phi) = \frac{V_m}{2} \{x(1-\cos\phi) + (1-x)(1-\cos 3\phi)\} \qquad (2)$$

where V_m($=4.1$ kcal/mole) is the height of the potential barrier, and x($=0.25$) is the weighting factor of the trans-conformation relative to the gauche. Temperature was maintained at $298°K$ throughout the simulation.

In order to fix the bond length and bond angle, the constraint equation of motion must be solved. Memon et al.[12] have developed the new algorithm which is the reliable, efficient and accurate one. We take this new efficient method to solve the constraint equation of a chain molecule. Other techniques in the MD simulation are the same as in the previous works.[9-11]

We have employed a different number (10,15 and 20) of chain elements in order to observe the effect of chain lengths on physical properties.

Note: All the quantities in this paper are expressed in reduced units as in our previous works.[9-11] Time in $[m(\alpha-6)/6\varepsilon\alpha]^{1/2}$; length in r_m; velocity in $[6\varepsilon\alpha/m(\alpha-6)^{1/2}$; temperature in ε/k; and density $\rho = N/(L/r_m)$, L being the length of the box.

Results and Discussions

Pair Correlation Functions. We calculated the pair correlation function g(r) to obtain information on the local structure of the system. If n(r) particles are situated at a distance between r and $r+\Delta r$ from a reference particle, the pair correlation function g(r) is given by,

$$g(r) = \frac{<n(r)>}{4\pi r^2 \rho \Delta r} \qquad (3)$$

where ρ is the number density($= N/V$) of the system. We use eq (3) to compute the pair correlation functions for solvent molecule-chain element (SC) and chain element-chain element (CC) pairs.

The calculated pair correlation function $g_{sc}(r)$ are shown in Figure 1. $g_{sc}(r)$ is proportional to the average probability of finding solvent molecules at distance r from a chain element in the chain, and it gives information on the distribution of the solvent molecules around the chain element. From Figure 1, we note that the features of the $g_{sc}(r)$ are a similar in all cases, i.e., the $g_{sc}(r)$'s are almost equal irrespective of the chain length($= N_c$) difference. This means that the $g_{sc}(r)$ is dependent on the movement of the particle, i.e., temperature of the system. This result ascertains the conclusion in our previous work,[10,11] i.e., $g_{sc}(r)$ is very sensitive to the temperature of system, but is weakly sensitive to the rotational barrier or the models used to represent the chain. Lee and Ree[8] reported a similar fact as to the N independence of $g_{sc}(r)$.

Next we turn our attention to the $g_{cc}(r)$. The $g_{cc}(r)$ is proportional to the possibility of finding the chain elements at
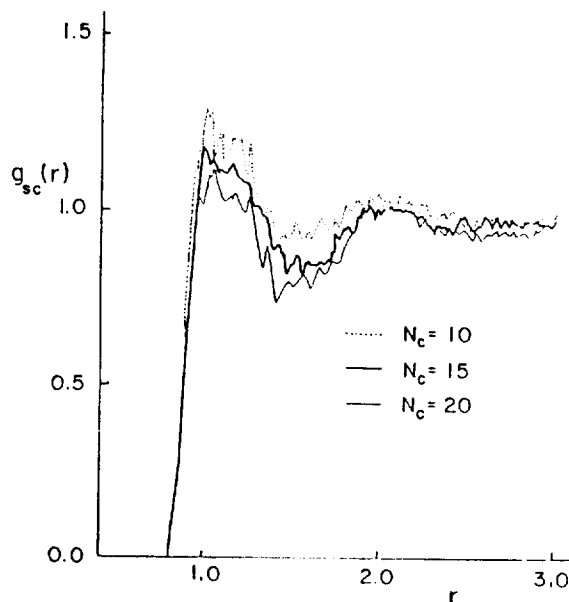

Figure 1. Pair correlation function $g_{sc}(r)$ between solvent molecules and the chain element vs. reduced distance r for the chains with different numbers of chain elements.
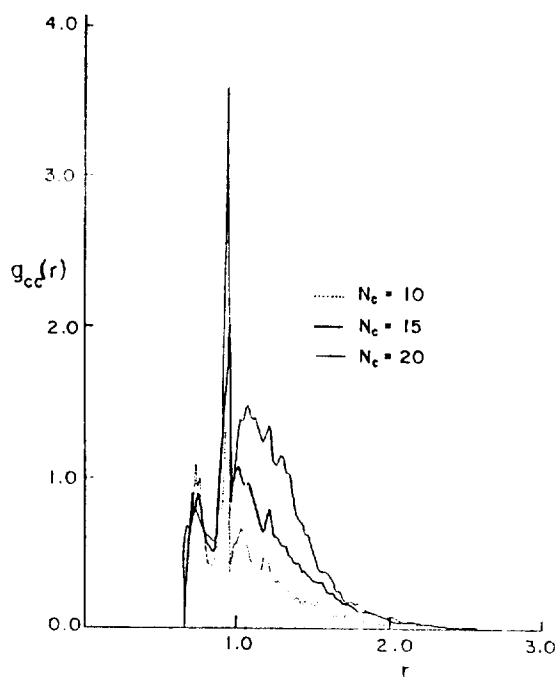

Figure 2. Pair correlation function $g_{cc}(r)$ between chain elements vs. reduced distance r for the chains with different numbers of chain elements.

distance r from a reference chain element, and it is related to the configuration of the chain. Figure 2 exhibits the $g_{cc}(r)$'s at different values of N_c. Note that the whole appearences are similar each other but the magnitudes of $g_{cc}(r)$ are different in all cases. It is natural that the magnitude is larger at larger N_c. The similar appearance of $g_{cc}(r)$'s is due to the fact that all the cases have the same model and the same potential parameters, so the general feature of $g_{cc}(r)$ is dependent only on the temperature or the rotational potential.

We calculated the fraction $\chi(\phi)$ of the chain conformation

having the rotation angle ϕ. The results (Figure 3) show no special difference between the cases. This is also due to the insensitivity of $\chi(\phi)$ on the N_c.

Configurational Properties. The mean-square end-to-end distance $<R^2>$ and the mean-square radius of gyration $<S^2>$ of a chain molecule are given by

$$<R^2(t)> = <|\vec{r}_1(t) - \vec{r}_{N_c}(t)|^2> \qquad (4)$$

and

$$<S^2(t)> = <\frac{1}{N_c}\sum_{i=1}^{N_c}[\vec{r}_i(t) - \vec{r}_{cm}(t)]^2> \qquad (5)$$

where $<\ >$ denotes an average value over all possible configuration, $\vec{r}_1$, $\vec{r}_{N_c}$ and $\vec{r}_i$ are the position vectors of the first, last, and ith elements on the chain, respectively, and $\vec{r}_{cm}$ is the center-of-mass vector.

$$\vec{r}_{cm}(t) = \frac{1}{N_c}\sum_{i=1}^{N_c}\vec{r}_i(t) \qquad (6)$$

The $<R^2>$, $<S^2>$ and ratio $<R^2>/<S^2>$ values obtained are summarized in Table 1.

The $<R^2>$ and $<S^2>$ under the unperturbed state can be calculated by using the theoretical equations.[13a]

For a freely-jointed chain,

$$<R^2>_0 = n\, l^2 \qquad (7)$$

and

$$<S^2>_0 = \frac{(n+2)}{6(n+1)}\, n\, l^2 \qquad (8)$$

where n is the number of bonds and is defined as $n = N_c - 1$, l is the bond length, and the subscript zero represents the unperturbed state.

For a freely rotating chain,

$$<R^2>_0 = n\, l^2\left[\frac{1+\alpha}{1-\alpha} - \frac{2\alpha}{n}\frac{1-\alpha^n}{(1-\alpha)^2}\right] \qquad (9)$$

and

$$<S^2>_0 = n\, l^2\left[\frac{(n+2)(1+\alpha)}{6(n+1)(1-\alpha)} - \frac{\alpha}{(n+1)(1-\alpha)^2}\right.$$
$$\left. + \frac{2\alpha^2}{(n+1)^2(1-\alpha)^3} - \frac{2\alpha^3(1-\alpha^n)}{n(n+1)^2(1-\alpha)^4}\right] \qquad (10)$$
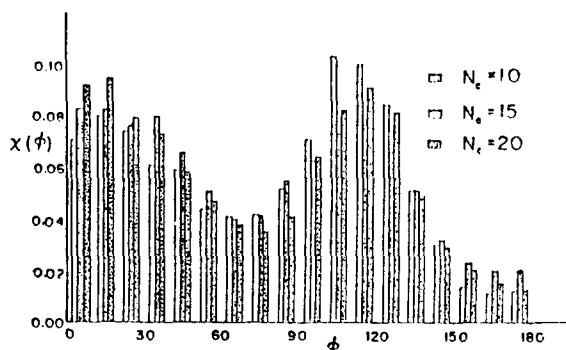

Figure 3. Fraction $\chi(\phi)$ of the conformers with rotation angle ϕ for the chains with different numbers of chain elements.

Table 1. Configurational Properties of n-Alkane Chain Molecules Depending on the Number of Chain Elements[a]

Properties		10	15	20
FJ[b]	$<R^2>$	1.210	1.882	2.554
	$<S^2>$	0.222	0.335	0.447
	$<R^2>/<S^2>$	5.455	5.625	5.714
FR[c]	$<R^2>$	2.402	3.880	5.357
	$<S^2>$	0.385	0.624	0.867
	$<R^2>/<S^2>$	6.245	6.212	6.177
HR[d]	$<R^2>$	2.927	5.226	7.546
	$<S^2>$	0.435	0.772	1.129
	$<R^2>/<S^2>$	6.732	6.777	6.682
MD	$<R^2>$	3.330 ± 0.581	3.560 ± 0.946	4.970 ± 0.728
	$<S^2>$	0.472 ± 0.035	0.677 ± 0.062	0.794 ± 0.067
	$<R^2>/<S^2>$	7.055	5.258	6.259
	$<\cos\phi>$[e]	0.1457	0.1843	0.1979
	$<S_1^2>/<S^2>$	0.290	0.271	0.274
	$<S_2^2>/<S^2>$	0.337	0.324	0.346
	$<S_3^2>/<S^2>$	0.373	0.405	0.380

[a]The value of $<R^2>$ and $<S^2>$ are reduced values. [b]FJ means the freely-jointed chain model in unperturbed state. $<R^2>$ and $<S^2>$ are calculated from eqs.(7) and (8), respectively. [c]FR means the freely rotating chain model. $<R^2>$ and $<S^2>$ are obtained from eqs. (9) and (10). [d]HR means the hindered rotating chain model. $<R^2>$ and $<S^2>$ are calculated from eqs.(11) and (14). [e]$<\cos\phi>$ is represented as a mean value of the dihedral angle ϕ.

where $\alpha = \cos\theta = \cos 68°$.[13b]

For a hindered rotating chain, if $\eta = <\cos\phi>$, then

$$<R^2>_0 = n\, l^2\left[\left(\frac{1+\alpha}{1-\alpha}\right)\left(\frac{1+\eta}{1-\eta}\right) - \left(\frac{\alpha\eta+\lambda_1}{\lambda_1-\lambda_2}\right)P_1\right.$$
$$\left. + \left(\frac{\alpha\eta+\lambda_2}{\lambda_1-\lambda_2}\right)P_2\right] \qquad (11)$$

where

$$P_k = \frac{2\lambda_k}{n}\frac{1-\lambda_k^n}{(1-\lambda_k)^2},\quad k = 1, 2 \qquad (12)$$

$$\lambda_{1,2} = \frac{1}{2}\left[\alpha(1-\eta) \pm \sqrt{\alpha^2(1-\eta)^2+4\eta}\right] \qquad (13)$$

and

$$<S^2>_0 = n\, l^2\left[\frac{1}{6}\left(\frac{n+2}{n+1}\right)\left(\frac{1+\alpha}{1-\alpha}\right)\left(\frac{1+\eta}{1-\eta}\right)\right.$$
$$\left. - \left(\frac{\alpha\eta+\lambda_1}{\lambda_1-\lambda_2}\right)Q_1 + \left(\frac{\alpha\eta+\lambda_2}{\lambda_1-\lambda_2}\right)Q_2\right] \qquad (14)$$

where

$$Q_k = \frac{\lambda_k}{(n+1)(1-\lambda_k)^2} - \frac{2\lambda_k^2}{(n+1)^2(1-\lambda_k)^3}$$
$$+ \frac{2\lambda_k^3(1-\lambda_k^n)}{n(n+1)^2(1-\lambda_k)^4} \qquad (15)$$

The values obtained from eqs.(7) through (14) are also shown in Table 1. The differences between the theoretical values calculated from these equations and the results from the MD calculation are pretty large. For a hinderd rotating chain, eqs.(11) and (14) are concerned with the short range effects determined overwhelmingly by interactions between groups separated by only a few bonds. Our MD simulation uses the same hindered rotational potential, but included the long range volume effects dominated by interactions between pairs which are separated by many bonds. This is the main reason for the discrepancy between these two values. For a definitive conclusion, however, more computation times are required which is beyond our resource at present.

The moment-of-inertia tensor T_{ab}, whose eigenvalues provide a rough estimate of the shape of the chain, is defined as[14]

$$T_{ab} = \frac{1}{N_c} \sum_{i=1}^{N_c} (\vec{r}_i - \vec{r}_{cm})_a (\vec{r}_i - \vec{r}_{cm})_b \qquad (16)$$

The eigenvalues $\langle S_i^2 \rangle / \langle S^2 \rangle$ (i = 1,2, and 3) reduce to 1/3 in the case of sphere, and the deviation from 1/3 indicates asphericity. The results are summarized in Table 1. From these results, it is found that the spatial configuration of the chain molecule has a spherical shape, and that the shape is not altered in any noticeable way by the variation in the number of chain elements. This conclusion accords also with the other workers' results.[5,6,8]

We obtained the distribution function of the end-to-end distance W(r). This value is shown in Figure 4 where the MD calculated values are compared with the values obtained from eq (17),[15]

$$W(r) = 4\pi r^2 \left(\frac{3}{2\pi \langle r^2 \rangle} \right)^{3/2} \exp\left(-\frac{3r^2}{2\langle r^2 \rangle} \right) \qquad (17)$$

where r is the end-to-end distance.

Equation (17) is based on the model of the random-flight chain, so the result from eq (17) is different from that of the MD calculation. One notes that the latter result deviates from
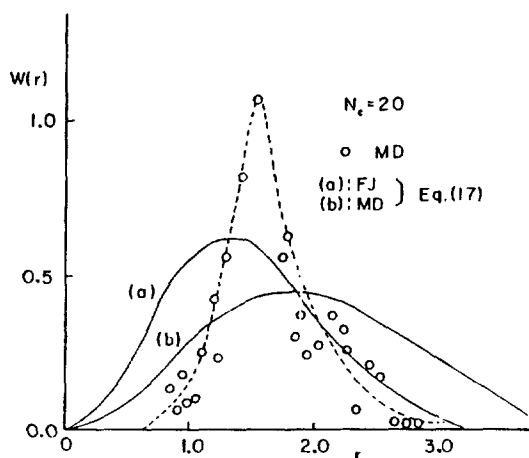
the Gaussian nature eq (17) since the model of the MD calculations is a hindered rotating chain.

Chain Relaxation Phenomena. We calculated the time dependent autocorrelation functions for the square end-to-end distance and for the square radius of gyration by using eq (18),[16]

$$C(A; k\Delta t) = \{(n-k) \sum_{i=1}^{n-k} A(l\Delta t) A[(l+k)\Delta t]$$

$$- \sum_{i=1}^{n-k} A(l\Delta t) \sum_{i=1}^{n-k} A[(l+k)\Delta t]\} \{(n-k) \sum_{i=1}^{n-k} A^2(l\Delta t)$$

$$- [\sum_{i=1}^{n-k} A(l\Delta t)]^2\}^{-1/2} \{(n-k) \sum_{i=1}^{n-k} A^2[(l+k)\Delta t]$$

$$-(\sum_{i=1}^{n-k} A[(l-k)\Delta t])^2\}^{-1/2} \qquad (18)$$

where k and l are integers, n being the total number of time steps taken for the averaging procedure. We choose $A(l\Delta t)$ to represent either R^2 or S^2 at time $t = l\Delta t$. The results are shown in Figure 5 and 6. One sees from Figure 5 and 6 that $C(R^2;t)$ and $C(S^2;t)$ of lower N_c decay faster than those of higher N_c. This comes from the fact that the longer chain relaxes slowly because of the larger dimension. These phenomena have also been observed by many authors.[5,6,17]

Next we calculate the velocity autocorrelation function (VACF) $C(\vec{V};t)$ of the center of mass using eq (19),

$$C(\vec{V}; t) = \langle \vec{V}(t) \vec{V}(t+k\Delta t) \rangle / \langle \vec{V}^2(t) \rangle \qquad (19)$$

The results are shown in Figure 7. It is noted that the $C(V;t)$ of the center of mass in the chain is weakly dependent on the
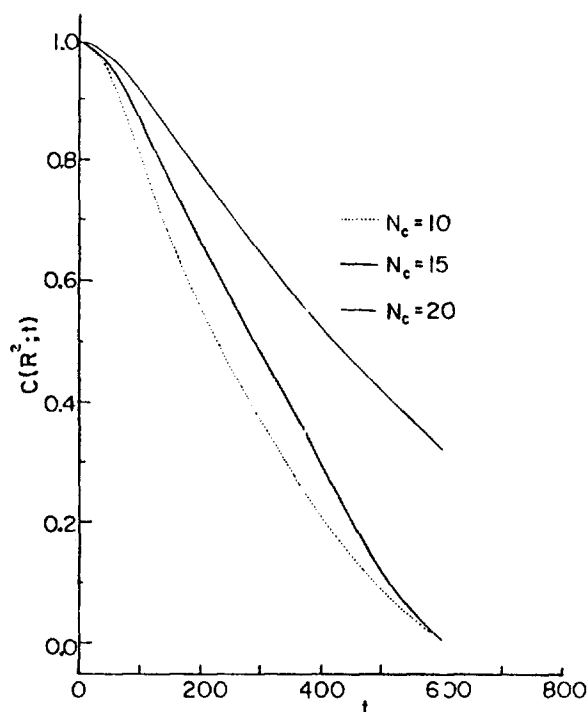

Figure 4. Distribution function of the end-to-end distance W(r) *vs.* reduced distance r for the chain of $N_c = 20$. The solid curves are the theoretical curves calculated from eq (17) on the assumption r = $\langle R^2 \rangle^{1/2}$. (a) R from the FJ model, and (b) R from the MD result (see Table 1). Dash-line curve is the MD simulation.

Figure 5. Autocorrelation function of the square end-to-end distance $C(R^2;t)$ *vs.* time for the chains with different numbers of chain elements. The time axis is shown in units of reduced t.

N_c for the chains of $N_c = 15$ and 20. The longer chain moves slowly since the dimension of the longer chain is larger. So the velocity does not change so much in the longer chains. This is the reason for the slow decaying of the VACF in the longer chains. Bishop *et al.*[5] also observed a similar tendency.

The translational motion of the chain has been monitored by calculating the diffusion coefficient D_c for the center of the mass and D_e for the end point by using eq (20),

$$D = \frac{1}{6} \lim_{t \to \infty} \frac{<r(t)^2>}{t} \qquad (20)$$

All the results are summarized in Table 2. It is noted that larger molecules have a smaller D_c. It is natural that the dif-
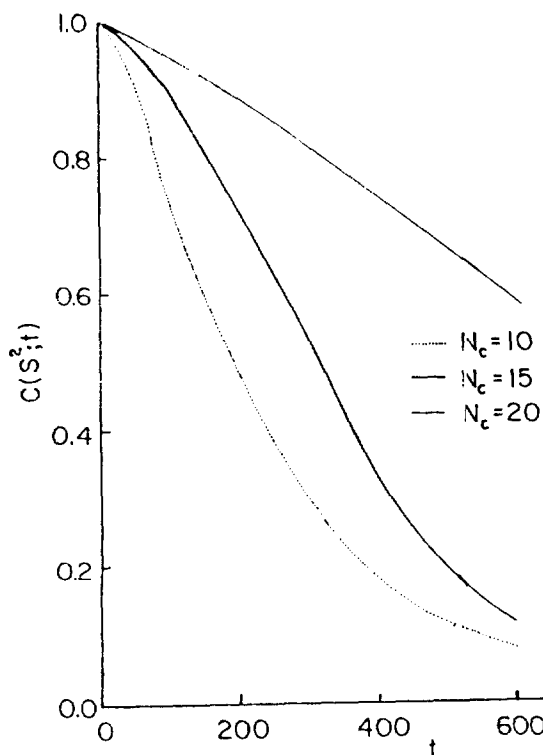

Figure 6. Autocorrelation function of the square radius of gyration $C(S^2;t)$ vs. time for the chains with different numbers of chain elements. The time axis is shown in units of reduced t.
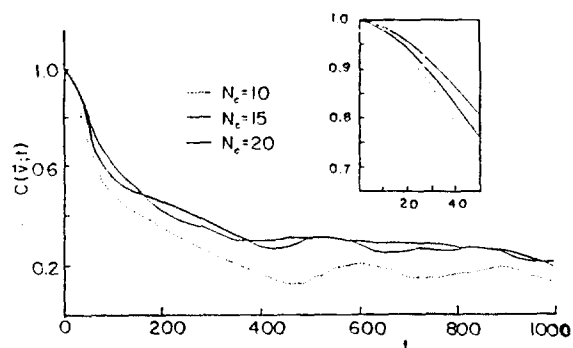

Figure 7. Velocity autocorrelation function $C(\bar{V};t)$ of the center of mass for the chains with different numbers of chain elements. The time axis is shown in units of reduced t.

Table 2. Diffusion Constant Depending on the Number of Chain Elements

diffusion constant	10	15	20
$D_c \times 10^5 (\text{cm}^2/\text{sec})^a$	8.611 ± 0.292	6.029 ± 0.208	3.489 ± 0.104
$D_e \times 10^4 (\text{cm}^2/\text{sec})^b$	1.572 ± 0.050	1.781 ± 0.032	1.568 ± 0.015

[a]D_c represents the diffusion constant of the center of mass of the chain molecule. [b]D_e represents the diffusion constant of the end point of the chain molecule.

fusion constant of the center of mass is smaller for the longer chains since the longer chain has larger dimensions.

Ceperly *et al.*[3] found that the diffusion constant is proportional to N_c^{-1}. The diffusion coefficients of the end-point D_e, however, are all nearly equal, irrespective of N_c (see Table 2.). While the diffusion coefficient of the center of mass D_c representes the whole motion of the chain, the diffusion coefficient D_c representes the motion of one element of the chain at the end point. The D_e independency of N_c is explained by the fact that the movement of the end point is dependent on the system-temperature and not on the length of the chain. The D_e values are larger than those of D_c. This is due to the fact that the end-point has a larger degree of freedom than the center of mass.

References

1. A. Baumgärtner, *J. Chem. Phys.*, **72**, 871 (1980).
2. S.D. Stellman and P.J. Gans, *Macromolecules*, **5**, 516 (1972).
3. D. Ceperley, M.H. Kalos, and J.L. Lebowitz, *Phys. Rev. Lett.*, **41**, 313 (1978).
4. P.H. Verdier and W.H. Stockmayer, *J. Chem. Phys.*, **36**, 227 (1962).
5. M. Bishop, M.H. Kalos, and H.L. Frisch, *J. Chem. Phys.*, **70**, 1299 (1979).
6. D.C. Rapaport, *J. Chem. Phys.*, **71**, 3299 (1979).
7. D.C. Rapaport, *J. Phys.*, **A11**, L213 (1978).
8. Y.S. Lee and T. Ree, *Bull. Korean Chem. Soc.*, **3**, 44 (1982).
9. S.H. Jeon, I.J. Oh and T. Ree, *J. Phys. Chem.*, **87**, 2890 (1983).
10. I.J. Oh and T. Ree, *Bull. Korean Chem. Soc.*, **51**, 162 (1984).
11. I.J. Oh and T. Ree, *J. Phys. Chem.*, **88**, 4 (1984).
12. M.K. Memon, R.W. Hookney, and S.K. Mitra, *J. Comput. Phys.*, **43**, 345 (1981).
13. P.J. Flory, "Statistical Mechanics of Chain Molecules," Interscience, New York, 1969, (a) Chap. 1,2, (b) p. 141.
14. K. Solc, *J. Chem. Phys.*, **55**, 335 (1971).
15. C. Tanford, "Physical Chemistry of Macromolecules," John Wiley & Sons, New York, 1961, p. 170-179.
16. W. Bruns and R. Bansal, *J. Chem. Phys.*, **74**, 2064 (1981).
17. D.E. Krabuehl and P.H. Verdier, *J. Chem. Phys.*, **67**, 361 (1977).